

ViLT: Vision-and-Language Transformer Without Convolution or Region Supervision

Wonjae Kim^{*1} Bokyoung Son^{*2} Ildoo Kim³

Abstract

Vision-and-Language Pretraining (VLP) has improved performance on various joint vision-and-language downstream tasks. Current approaches to VLP heavily rely on image feature extraction processes, most of which involve region supervision (e.g., object detection) and the convolutional architecture (e.g., ResNet). Although disregarded in the literature, we find it problematic in terms of both (1) efficiency/speed, that simply extracting input features requires much more computation than the multimodal interaction steps; and (2) expressive power, as it is upper bounded to the expressive power of the visual encoder and its predefined visual vocabulary. In this paper, we present a minimal VLP model, Vision-and-Language Transformer (ViLT), monolithic in the sense that processing of visual inputs is drastically simplified to just the same convolution-free manner that we process textual inputs. We show that ViLT is up to 60 times faster than previous VLP models, yet with competitive or better downstream task performance.

1. Introduction

The pretrain-and-finetune scheme has been expanded to a joint domain of vision and language, giving birth to the category of *Vision-and-Language Pretraining (VLP)* models (Lu et al., 2019; Chen et al., 2019; Su et al., 2019; Li et al., 2019; Tan & Bansal, 2019; Li et al., 2020a; Lu et al., 2020; Qi et al., 2020; Zhou et al., 2020; Huang et al., 2020; Li et al., 2020b; Gan et al., 2020; Yu et al., 2020; Zhang et al., 2021). These models are pretrained with image text match-

^{*}Equal contribution ¹Kakao Corporation, Pangyo, Seongnam, Republic of Korea ²Kakao Enterprise, Pangyo, Seongnam, Republic of Korea ³Kakao Brain, Pangyo, Seongnam, Republic of Korea. Correspondence to: Wonjae Kim <dan-delin.kim@kakaocorp.com>.

²See Section 4.3 for complexity analysis of VLP models.

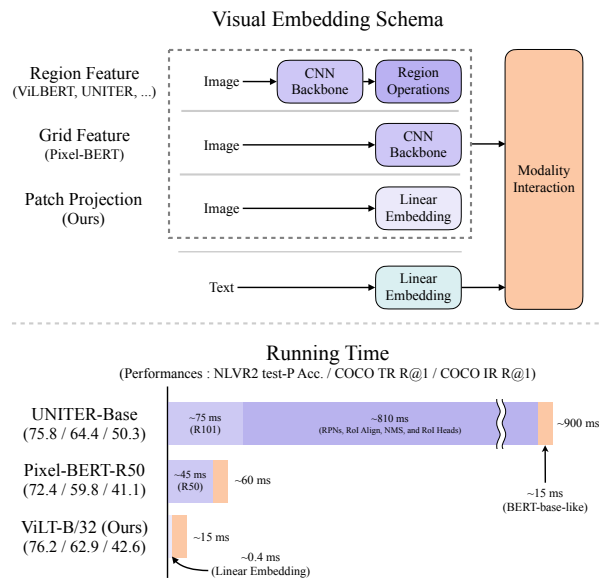


Figure 1. Visual comparison of conventional VLP architectures and our proposed ViLT. We have completely removed convolutional neural networks from the VLP pipeline without hurting performance on downstream tasks. ViLT is the first VLP model of which the modal-specific components require *less* computation than the transformer component for multimodal interactions².

ing and masked language modeling objectives³ on images and their aligned descriptions, and are finetuned on vision-and-language downstream tasks where the inputs involve two modalities.

In order to be fed into VLP models, image pixels need to be initially embedded in dense form alongside language tokens. Deep convolutional networks have been widely regarded essential for this visual encoding step since the seminal work of Krizhevsky et al. (2012). Most VLP models employ an object detector pretrained on the Visual Genome dataset (Krishna et al., 2017) annotated with 1,600 object classes and 400 attribute classes as in Anderson et al. (2018). Pixel-BERT (Huang et al., 2020) is one exception, as it uses ResNet variants (He et al., 2016; Xie et al., 2017) pretrained on ImageNet classification (Russakovsky et al.,

³While some work employ additional objectives and data structures, these two objectives apply to almost every VLP model.

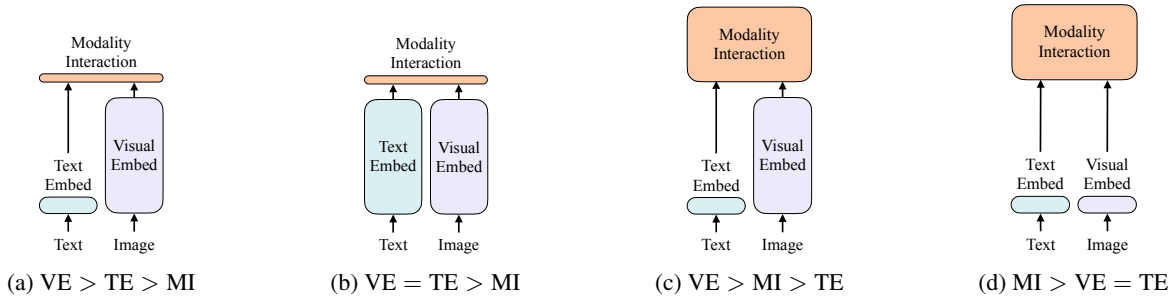


Figure 2. Four categories of vision-and-language models. The height of each rectangle denotes its relative computational size. VE, TE, and MI are short for visual embedding, text embedding, and modality interaction, respectively.

2015) instead of object detection modules.

To this date, most work have focused on improving performance through increasing the power of visual embedders. The shortcomings of having a heavy visual embedder is often disregarded in academic experiments, because region features are commonly cached in advance to ease the burden of feature extraction on training time. However, the limitations are still evident in real-world applications as the queries in the wild have to undergo the slow extraction process.

To this end, we shift our attention on lightweight and fast encoding of visual inputs. Recent work (Dosovitskiy et al., 2020; Touvron et al., 2020) demonstrated that using a simple linear projection of a patch is effective enough to embed pixels before feeding them into transformers. Whereas being the solid mainstream for text (Devlin et al., 2018), it is only recently that transformers (Vaswani et al., 2017) are used for images as well. We presume that the transformer module—used for modality interaction in VLP models—can also manage to process visual features in place of a convolutional visual embedder, just as it processes textual features.

In this paper, we propose the Vision-and-Language Transformer (ViLT) that handles two modalities in a single unified manner. It mainly differs from previous VLP models in its shallow, convolution-free encoding of pixel-level inputs. Removing deep encoders solely dedicated to visual inputs significantly cuts down the model size and running time by design. Figure 1 shows that our parameter-efficient model is 60 times faster than VLP models with region features and 4 times faster than those with grid features, while exhibiting similar or even better performance on vision-and-language downstream tasks.

Our key contributions can be summarized as follows:

- ViLT is the *simplest possible* architecture for a vision-and-language model as it commissions the transformer module to extract and process visual features in place of a separate deep visual encoder. This design inherently leads to significant parameter and runtime effi-

ciency.

- For the first time, we achieve competent performance on vision-and-language tasks without using region features or deep convolutional visual encoders in general.
- Also for the first time, we empirically show that whole word masking and image augmentations that were unprecedented in VLP training schemes further drive performance.

2. Background

2.1. Taxonomy of Vision-and-Language Models

We propose a taxonomy of vision-and-language models based on two points: (1) whether the two modalities have an even level of expressiveness in terms of dedicated parameters and/or computation; and (2) whether the two modalities interact in a deep network. This leads to four archetypes in Figure 2.

The *visual semantic embedding* (VSE) models such as VSE++ (Faghri et al., 2017) and SCAN (Lee et al., 2018) belong to Figure 2a. They use separate encoders for image and text, with the former being much heavier, then represent the similarity of the encoded features from the two modalities with simple dot products or shallow attention layers.

CLIP (Radford et al., 2021) belongs to Figure 2b as it uses separate but equally expensive transformer encoders for each modality. Interaction between the pooled image vector and text vector is still shallow (dot product). Despite CLIP’s remarkable zero-shot performance on image-to-text retrieval, we could not observe the same level of performance on other vision-and-language downstream tasks. For instance, if we use the dot product of pooled visual and textual vectors from CLIP as the multimodal representation, the NLVR2 (Suhr et al., 2018) dev accuracy is only 50.99 ± 0.38 ; since chance level accuracy is 0.5, we conclude that the representations are incapable of learning this task. This result also matches the findings of Suhr et al. (2018) that all models with simply fused multimodal representation

(Hu et al., 2017; Perez et al., 2018; Hudson & Manning, 2018) failed to learn NLVR2. This backs up our speculation that simple fusion of outputs even from high-performing unimodal encoders may not be sufficient to learn complex vision-and-language tasks, buttressing the need for a more rigorous inter-modal interaction scheme.

Unlike models with shallow interaction, the more recent VLP models that fall under Figure 2c use a deep transformer to model the interaction of image and text features. Aside from the interaction module, however, convolutional networks are still involved in extracting and encoding image features. This accounts for most of the computation as in Figure 1.

Our proposed ViLT is the first model of type Figure 2d where the embedding layers of raw pixels are shallow and computationally light as of text tokens. This architecture thereby concentrates most of the computation to modeling modality interactions.

2.2. Modality Interaction Schema

At the very core of contemporary VLP models lie transformers. They get image and text embedding sequences as input, model inter-modal and optionally intra-modal interactions throughout layers, then output a contextualized feature sequence.

Bugliarello et al. (2020) classifies interaction schema into two categories: (1) *single-stream* approaches (e.g., VisualBERT (Li et al., 2019), UNITER (Chen et al., 2019)) where layers collectively operate on a concatenation of image and text inputs; and (2) *dual-stream* approaches (e.g., ViLBERT (Lu et al., 2019), LXMERT (Tan & Bansal, 2019)) where the two modalities are not concatenated at the input level. We follow the single-stream approach for our interaction transformer module, because the dual-stream approach introduces additional parameters.

2.3. Visual Embedding Schema

Whereas all performant VLP models share the same text embedder⁴, they differ on visual embedders. Still in most (if not all) cases, visual embedding is the bottleneck of existing VLP models. We focus on cutting corners on this step by introducing patch projection instead of using region or grid features for which heavy extraction modules are used.

Region Feature. Region features are dominantly utilized among VLP models. They are obtained from an off-the-shelf object detector such as Faster R-CNN (Ren et al., 2016) typically pretrained on the Visual Genome (VG) dataset processed by Anderson et al. (2018).

⁴Tokenizer from pretrained BERT, word and position embeddings parameters resembles those of BERT.

A region proposal network proposes several thousands of regions of interest (RoIs) based on the grid features pooled from the CNN backbone. Non-maximum suppression (NMS) then reduces the number of RoIs to 1~2K. After being pooled by operations such as RoI Align (He et al., 2017), the RoIs go through RoI heads and become region features. NMS is again applied to every class, finally reducing the number of features under 100. This per-class non-parallel NMS becomes a substantial runtime bottleneck. This problem is aggravated especially with a large number of classes (e.g., 1,600 in the VG dataset). Freezing the visual backbone and caching the region features in advance only helps training time and not inference, not to mention that it could hold performance back.

VLP models with region features typically use ResNet-101 (Lu et al., 2019; Tan & Bansal, 2019; Su et al., 2019) or ResNext-152 (Li et al., 2019; 2020a; Zhang et al., 2021) as their CNN backbones. While the choice of the backbone clearly affects performance, previous works were lenient with controlling the capacity of visual embedders.⁵ For a fairer comparison, we report inference time along with performance.

Grid Feature. Direct use of grid features without region supervision was first proposed by VQA-specific models (Jiang et al., 2020; Nguyen et al., 2020). This was mainly to avoid using severely slow region selection operations.

Aside from task-specific models, Pixel-BERT is the only VLP model that used grid features. It used CNNs pretrained with ImageNet classification and tuned during vision-and-language pretraining. Grid features from the CNNs are directly fed into the modality interaction transformer. Pixel-BERT falls below region feature based models with ResNet-50, but with a much heavier ResNeXt-152 its performance moves up to its competitors.

We claim that grid features are not the go-to option, however, since CNNs are still expensive that they account for a large portion of the whole computation as in Figure 1.

Patch Projection. To minimize overhead, we adopt the simplest visual embedding scheme: *linear projection* that operates on image patches. The patch projection embedding was introduced by ViT (Dosovitskiy et al., 2020) for image classification tasks. Patch projection drastically simplifies the visual embedding step to the level of textual embedding, which also consists of simple projection (lookup) operations. In comparison with complex ResNe(X)t backbones,⁶ a 32×32 patch projection only requires 2.4M parameters. Its running time is also ignorable as in Figure 1.

⁵Bugliarello et al. (2020) showed that a controlled setup bridges the performance gap of various region feature based VLP models.

⁶Parameters for R50 is 25M, R101 is 44M, and X152 is 60M.

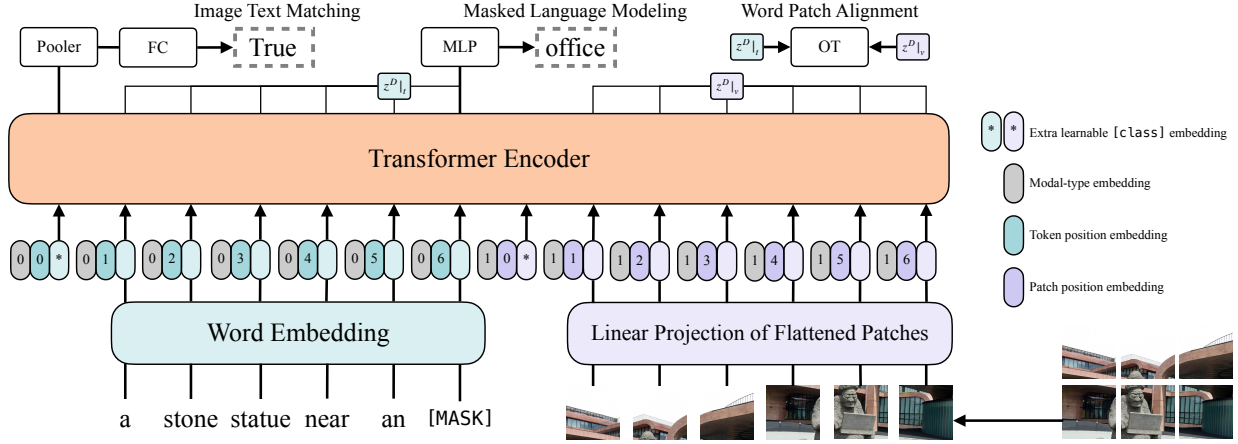


Figure 3. Model overview. The illustration was inspired by Dosovitskiy et al. (2020)

3. Vision-and-Language Transformer

3.1. Model Overview

With a minimal visual embedding pipeline and following the single-stream approach, ViLT has the simplest architecture possible for a VLP model.

We deviate from the literature that we initialize the interaction transformer weights from pretrained ViT instead of BERT. This is to exploit the power of the interaction layers to process visual features while lacking a separate deep visual encoder.⁷

$$\bar{t} = [t_{\text{class}}; t_1 T; \dots; t_L T] + T^{\text{pos}} \quad (1)$$

$$\bar{v} = [v_{\text{class}}; v_1 V; \dots; v_N V] + V^{\text{pos}} \quad (2)$$

$$z^0 = [\bar{t} + t^{\text{type}}; \bar{v} + v^{\text{type}}] \quad (3)$$

$$\hat{z}^d = \text{MSA}(\text{LN}(z^{d-1})) + z^{d-1}, \quad d = 1 \dots D \quad (4)$$

$$z^d = \text{MLP}(\text{LN}(\hat{z}^d)) + \hat{z}^d, \quad d = 1 \dots D \quad (5)$$

$$p = \tanh(z_0^D W_{\text{pool}}) \quad (6)$$

The ViT encoder consists of stacked blocks that include a multiheaded self-attention (MSA) layer and a MLP layer. The position of layer normalization (LN) in ViT is the only difference from BERT: LN comes after MSA and MLP in BERT (“post-norm”), and before in ViT (“pre-norm”).

The input text $t \in \mathbb{R}^{L \times |V|}$ is embedded to $\bar{t} \in \mathbb{R}^{L \times H}$ with a word embedding matrix $T \in \mathbb{R}^{|V| \times H}$ and a position embedding matrix $T^{\text{pos}} \in \mathbb{R}^{(L+1) \times H}$.

The input image $I \in \mathbb{R}^{C \times H \times W}$ is sliced into patches and flattened to $v \in \mathbb{R}^{N \times (P^2 \cdot C)}$ where (P, P) is the patch resolution and $N = HW/P^2$. Followed by linear projection $V \in \mathbb{R}^{(P^2 \cdot C) \times H}$ and position embedding $V^{\text{pos}} \in \mathbb{R}^{(N+1) \times H}$, v is embedded into $\bar{v} \in \mathbb{R}^{N \times H}$.

⁷Training with pretrained patch projection from ViT and pretrained BERT for the interaction module did not work.

The text and image embeddings are summed with their corresponding modal-type embedding vectors $t^{\text{type}}, v^{\text{type}} \in \mathbb{R}^H$, then are concatenated into a combined sequence z^0 . The contextualized vector z is iteratively updated through D -depth transformer layers up until the final contextualized sequence z^D . p is a pooled representation of the whole multimodal input, and is obtained by applying linear projection $W_{\text{pool}} \in \mathbb{R}^{H \times H}$ and hyperbolic tangent upon the first index of sequence z^D .

For all experiments, we use weights from ViT-B/32 pretrained on ImageNet, hence the name ViLT-B/32.⁸ Hidden size H is 768, layer depth D is 12, patch size P is 32, MLP size is 3,072, and the number of attention heads is 12. The total number of parameters is 86M.

3.2. Pretraining Objectives

We train ViLT with two objectives: masked language modeling (MLM) and image text matching (ITM), which are commonly used to train VLP models.

Image Text Matching. We randomly replace the aligned image to a different image with the probability of 0.5. A single linear layer ITM head projects the pooled output feature p to logits over binary class, and we compute negative log likelihood loss as our ITM loss.

Plus, inspired by the word region alignment objective in Chen et al. (2019), we design word patch alignment (WPA) that computes the alignment score between two subsets of z^D : $z^D|_t$ (textual subset) and $z^D|_v$ (visual subset), using the inexact proximal point method for optimal transports (IPOT) (Xie et al., 2020). We set the hyperparameters of

⁸ViT-B/32 is pretrained with ImageNet-21K and finetuned on ImageNet-1K for image classification. We expect that weights pretrained on larger datasets (e.g., JFT-300M) would yield better performance.

IPOT following [Chen et al. \(2019\)](#) ($\beta = 0.5, N = 50$), and add the approximate wasserstein distance multiplied by 0.1 to the ITM loss.

Masked Language Modeling. This objective is to predict the ground truth labels of masked text tokens t_{masked} from its contextualized vector $z_{\text{masked}}^D|t$. Following the heuristics of [Devlin et al. \(2018\)](#), we randomly mask t with the probability of 0.15. We use a two layer MLP MLM head that inputs $z_{\text{masked}}^D|t$ and outputs logits over vocabulary, just as the MLM objective of BERT. The MLM loss is then computed as the negative log likelihood loss for the masked tokens.

3.3. Whole Word Masking

Whole word masking is a masking technique that masks all consecutive subword tokens that compose a whole word. It is shown to be effective on downstream tasks when applied to original and Chinese BERT ([Cui et al., 2019](#)).

We hypothesize that whole word masking is particularly crucial for VLP in order to make full use of information from the other modality. For example, the word “giraffe” is tokenized into three wordpiece tokens [“gi”, “##raf”, “##fe”] with the pretrained `bert-base-uncased` tokenizer. If not all tokens are masked, say, [“gi”, “[MASK]”, “##fe”], the model may solely rely on the nearby two language tokens [“gi”, “##fe”] to predict the masked “##raf” rather than using the information from the image. We mask whole words with a mask probability of 0.15 during pretraining. We discuss its impact in [Section 4.6](#).

3.4. Image Augmentation

Image augmentation reportedly improves generalization power of vision models ([Shorten & Khoshgoftaar, 2019](#)). DeiT ([Touvron et al., 2020](#)) that builds on ViT experimented with various augmentation techniques ([Zhang et al., 2017](#); [Yun et al., 2019](#); [Berman et al., 2019](#); [Hoffer et al., 2020](#); [Cubuk et al., 2020](#)), and found them beneficial for ViT training. However, the effects of image augmentation has not been explored within VLP models. Caching visual features restrains region feature based VLP models from using image augmentation. Notwithstanding its applicability, neither did grid feature based Pixel-BERT study its effects.

To this end, we apply RandAugment ([Cubuk et al., 2020](#)) during finetuning. We use all the original policies except two: color inversion, because texts often contain color information as well, and cutout, as it may clear out small but important objects dispersed throughout the whole image. We use $N = 2, M = 9$ as the hyperparameters. We discuss its impact in [Section 4.6](#) and [Section 5](#).

Table 1. Pretraining dataset statistics. Caption length is the length of tokens from pretrained `bert-base-uncased` tokenizer. † GCC and SBU provide only image urls, so we collect the images from urls which were still accessible.

Dataset	# Images	# Captions	Caption Length
MSCOCO	113K	567K	11.81 ± 2.81
VG	108K	5.41M	5.53 ± 1.76
GCC†	3.01M	3.01M	10.66 ± 4.93
SBU†	867K	867K	15.0 ± 7.74

4. Experiments

4.1. Overview

We use four datasets for pretraining: Microsoft COCO (MSCOCO) ([Lin et al., 2014](#)), Visual Genome (VG), SBU Captions (SBU) ([Ordonez et al., 2011](#)), and Google Conceptual Captions (GCC) ([Sharma et al., 2018](#)). [Table 1](#) reports the dataset statistics.

We evaluate ViLT on two widely explored types of vision-and-language downstream tasks: for *classification*, we use VQAv2 ([Goyal et al., 2017](#)) and NLVR2, and for *retrieval*, we use MSCOCO and Flickr30K (F30K) ([Plummer et al., 2015](#)) re-splited by [Karpathy & Fei-Fei \(2015\)](#). For the classification tasks, we finetune for three times with different initialization seeds for the head and data ordering, and report the max scores over all runs⁹. For the retrieval tasks, we only finetune once.

4.2. Implementation Details

For all experiments, we use AdamW optimizer ([Loshchilov & Hutter, 2017](#)) with base learning rate of 10^{-4} and weight decay of 10^{-2} . The learning rate was warmed up for 10% of the total training steps and was decayed linearly to zero for the rest of the training. Note that downstream performance may be further improved if we customize the hyperparameters to each task.

We resize the shorter edge of input images to 384 and limit the longer edge to under 640 while preserving the aspect ratio. This resizing scheme is also used during object detection in other VLP models, but with a larger size of the shorter edge (800). Patch projection of ViLT-B/32 yields $12 \times 20 = 240$ patches for an image with a resolution of 384×640 . As this is a rarely reached upper limit, we sample 200 patches for later processing. We interpolate V^{pos} of ViT-B/32 to fit the size of each image, and pad the patches to length 200 for batch training. Note that the resulting image resolution is four times smaller than $800 \times 1,333$ which is the size that all other VLP models use for inputs to their visual embedders.

⁹The mean and standard deviation is reported in [Table 5](#).

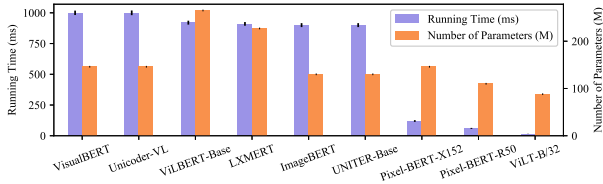


Figure 4. Running time and the number of parameters of various VLP models. Running time is averaged over 10K times on a single NVIDIA P40 GPU.

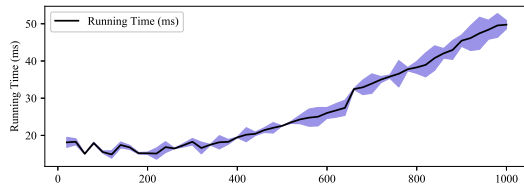


Figure 5. Running time of BERT-base-like transformer according to input sequence length.

We use the `bert-base-uncased` tokenizer for text inputs. Instead of finetuning from pretrained BERT, we learn the text embedding-related parameters t_{class} , T , and T^{pos} from scratch.

We pretrain for 100K steps (~ 3 days) on 64 NVIDIA V100 GPUs with a batch size of 4,096. For all downstream tasks, we train for 10 epochs with a batch size of 256 for VQAv2/retrieval tasks and 128 for NLVR2.

4.3. Complexity Analysis of VLP Models

Figure 4 reports the number of parameters in the visual embedder and transformer, plus the total running time throughout the whole pipeline, ViLT-B/32 being the best model in both terms. We also observe in Figure 5 that overhead accounts for most of the runtime of BERT-base-like transformer for sequences of length under 300. This keeps our model efficient despite its longer input sequence to the transformer module; image and text tokens combined, ViLT-B/32 and Pixel-BERT transformer receives ~ 280 tokens, while transformers in region feature based VLP models receive 76 \sim 140 tokens.¹⁰

4.4. Classification Tasks

We evaluate ViLT-B/32 on two commonly used datasets: VQAv2 and NLVR2. We use a two-layer MLP of hidden size 1,536 as the finetuned downstream head.

¹⁰Patch projection of ViLT-B/32 and grid features of Pixel-BERT result in at most 240 image tokens. Other models retrieve 36 \sim 100 image tokens as a result of object detection. The maximum text length is set to 40 tokens for all models.

Table 2. Comparison of ViLT-B/32 with other models on downstream classification tasks. We use MCAN (Yu et al., 2019) and MaxEnt (Suh et al., 2018) for VQAv2 and NLVR2 w/o VLP SOTA results. † additionally used GQA, VQAv2, VG-QA for pretraining. ‡ used open images dataset (Kuznetsova et al., 2020) to expand its visual vocabulary of region feature embeddings. @ indicates RandAugment is applied during finetuning.

Visual Embed	Model	Time (ms)	VQAv2 test-dev	NLVR2 dev	test-P
Region	w/o VLP SOTA	~ 900	70.63	54.80	53.50
	ViLBERT	~ 920	70.55	-	-
	VisualBERT-Base	~ 1000	70.80	67.40	67.00
	LXMERT	~ 910	72.42	74.90	74.50
	UNITER-Base	~ 900	72.70	75.85	75.80
	OSCAR-Base [†]	~ 900	73.16	78.07	78.36
	VinVL-Base [‡]	~ 1000	75.95	82.05	83.08
Grid	Pixel-BERT-X152	~ 120	74.45	76.50	77.20
	Pixel-BERT-R50	~ 60	71.35	71.70	72.40
Linear	ViLT-B/32	~ 15	70.34	74.56	74.66
	ViLT-B/32@	~ 15	70.94	75.24	76.21

Visual Question Answering. The VQAv2 task asks for answers given pairs of an image and a question in natural language. The annotated answers are originally in free-form natural language, but it is a common practice to convert the task to a classification task with 3,129 answer classes. Following this practice, we finetune ViLT-B/32 on VQAv2 train and validation sets while reserving 1,000 validation images and its related questions for internal validation. We report the test-dev score results¹¹ from the submission to the evaluation server. Note that we only use VQAv2 for finetuning while many other work also used VG-QA.

Natural Language for Visual Reasoning. The NLVR2 task is a binary classification task given triplets of two images and a question in natural language. As there are two input images unlike the pretraining setup, multiple strategies exist¹²; following OSCAR (Li et al., 2020b) and VinVL (Zhang et al., 2021), we use the *pair* method. Here, the triplet input is reformulated into two pairs: (question, image1) and (question, image2). The head takes the concatenation of two pooled representations (p).

Table 2 shows the results. ViLT-B/32 maintains competitive performance on both datasets considering its remarkable inference speed.

4.5. Retrieval Tasks

We finetune ViLT on the Karpathy & Fei-Fei (2015) split of MSCOCO and F30K. For image-to-text and text-to-image

¹¹VQA score is calculated by comparing the inferred answer to 10 ground truth answers: see <https://visualqa.org/evaluation.html> for details.

¹²UNITER proposed three downstream head setups: pair, triplet, and pair-biattn.

Table 3. Comparison of ViLT-B/32 with other VLP models on downstream zero-shot retrieval tasks. We exclude the models of which zero-shot retrieval performances were not reported in their original papers. † is pretrained with 10M proprietary image-text dataset in addition to 4M dataset of GCC+SBU.

Visual Embed	Model	Time (ms)	Zero-Shot Text Retrieval						Zero-Shot Image Retrieval					
			Flickr30k (1K)			MSCOCO (5K)			Flickr30k (1K)			MSCOCO (5K)		
			R@1	R@5	R@10	R@1	R@5	R@10	R@1	R@5	R@10	R@1	R@5	R@10
Region	ViLBERT-Base	~920	-	-	-	-	-	-	31.9	61.1	72.8	-	-	-
	Unicoder-VL	~1000	64.3	85.8	92.3	-	-	-	48.4	76.0	85.2	-	-	-
	UNITER-Base	~900	80.7	95.7	98.0	-	-	-	66.2	88.4	92.9	-	-	-
	ImageBERT†	~900	70.7	90.2	94.0	44.0	71.2	80.4	54.3	79.6	87.5	32.3	59.0	70.2
Linear	ViLT-B/32	~15	69.7	91.0	96.0	53.4	80.7	88.8	51.3	79.9	87.9	37.3	67.4	79.0

Table 4. Comparison of ViLT-B/32 with other models on downstream retrieval tasks. We use SCAN for w/o VLP SOTA results. † additionally used GQA, VQAv2, VG-QA for pretraining. ‡ used open images dataset to expand its visual vocabulary of region feature embeddings. @ indicates RandAugment is applied during finetuning.

Visual Embed	Model	Time (ms)	Text Retrieval						Image Retrieval					
			Flickr30k (1K)			MSCOCO (5K)			Flickr30k (1K)			MSCOCO (5K)		
			R@1	R@5	R@10	R@1	R@5	R@10	R@1	R@5	R@10	R@1	R@5	R@10
Region	w/o VLP SOTA	~900	67.4	90.3	95.8	50.4	82.2	90.0	48.6	77.7	85.2	38.6	69.3	80.4
	ViLBERT-Base	~920	-	-	-	-	-	-	58.2	84.9	91.5	-	-	-
	Unicoder-VL	~1000	86.2	96.3	99.0	62.3	87.1	92.8	71.5	91.2	95.2	48.4	76.7	85.9
	UNITER-Base	~900	85.9	97.1	98.8	64.4	87.4	93.1	72.5	92.4	96.1	50.3	78.5	87.2
	OSCAR-Base†	~900	-	-	-	70.0	91.1	95.5	-	-	-	54.0	80.8	88.5
	VinVL-Base†‡	~1000	-	-	-	74.6	92.6	96.3	-	-	-	58.1	83.2	90.1
Grid	Pixel-BERT-X152	~120	87.0	98.9	99.5	63.6	87.5	93.6	71.5	92.1	95.8	50.1	77.6	86.2
	Pixel-BERT-R50	~60	75.7	94.7	97.1	59.8	85.5	91.6	53.4	80.4	88.5	41.1	69.7	80.5
Linear	ViLT-B/32	~15	81.4	95.6	97.6	61.8	86.2	92.6	61.9	86.8	92.8	41.3	72.0	82.5
	ViLT-B/32@	~15	83.7	97.2	98.1	62.9	87.1	92.7	62.2	87.6	93.2	42.6	72.8	83.4

retrieval, we measure both zero-shot and finetuned performance¹³. We initialize the score head from the pretrained ITM head; in particular, the part that computes the true-pair logits. We sample 15 random texts as negative samples and tune the model with cross entropy loss that maximizes the scores on true pairs.

We report the zero shot retrieval results in Table 3 and finetuned results in Table 4. At zero-shot retrieval, ViLT-B/32 performs better in general than ImageBERT despite ImageBERT’s pretraining on a larger (14M) dataset. At finetuned retrieval, recalls for ViLT-B/32 are higher by a large margin than the second fastest model (Pixel-BERT-R50).

4.6. Ablation Study

In Table 5, we perform various ablations. More training steps, whole word masking and image augmentation come to be beneficial, whereas an additional training objective does not help.

It has been reported that the number of training iterations affect the performance of self-supervised models (Devlin et al., 2018; Chen et al., 2020a;b). As VLP is also a form of self-supervised training, we examine the effects of training durations. As expected, the performance constantly

¹³R@K corresponds to whether the ground truth is included among top K results from the validation set.

increases as we train the model for longer training steps (rows 1~3). Masking whole words for the MLM objective (rows 3~4) and finetuning with augmentation (row 6) also drive performance.

An additional masked region modeling (MRM) objective has been the key for performance boost in VLP models such as Chen et al. (2019). We experiment with masked patch prediction (MPP) (Dosovitskiy et al., 2020) which mimics the effect of MRM in a form compatible with patch projections. v is masked with the probability of 0.15, and the model predicts the mean RGB value of the masked patch from its contextualized vector $z_{\text{masked}}^D|_v$. However, MPP turns out not to be contributing to downstream performance (rows 4~5). This is in sharp contrast to the MRM objective on supervision signals from object detection.

4.7. Visualization

Figure 6 is an example of a cross-modal alignment. The transportation plan of WPA expresses a heatmap for a text token. Each square tile represents a patch, and its opacity indicates how much mass is transported from the highlighted word token.

More IPOT iterations (over 50 as in the training phase) help the visualization heatmap converge; empirically, 1,000 iterations are sufficient to get a clearly identifiable heatmap.

Table 5. Ablation study of ViLT-B/32. \textcircled{w} denotes whether whole word masking is used for pretraining. \textcircled{m} denotes whether MPP objective is used for pretraining. \textcircled{a} denotes whether RandAugment is used during finetuning.

Training Steps	Ablation			VQAv2		NLVR2		Flickr30k R@1 (1K)		MSCOCO R@1 (5K)	
	\textcircled{w}	\textcircled{m}	\textcircled{a}	test-dev	dev	test-P	TR (ZS)	IR (ZS)	TR (ZS)	IR (ZS)	
25K	X	X	X	68.96 \pm 0.07	70.83 \pm 0.19	70.83 \pm 0.23	75.39 (45.12)	52.52 (31.80)	53.72 (31.55)	34.88 (21.58)	
50K	X	X	X	69.80 \pm 0.01	71.93 \pm 0.27	72.92 \pm 0.82	78.13 (55.57)	57.36 (40.94)	57.00 (39.56)	37.47 (27.51)	
100K	X	X	X	70.16 \pm 0.01	73.54 \pm 0.02	74.15 \pm 0.27	79.39 (66.99)	60.50 (47.62)	60.15 (51.25)	40.45 (34.59)	
100K	O	X	X	70.33 \pm 0.01	74.41 \pm 0.21	74.57 \pm 0.09	81.35 (69.73)	61.86 (51.28)	61.79 (53.40)	41.25 (37.26)	
100K	O	O	X	70.21 \pm 0.05	72.76 \pm 0.50	73.54 \pm 0.47	78.91 (63.67)	58.76 (46.96)	59.53 (47.75)	40.08 (32.28)	
100K	O	X	O	70.85 \pm 0.13	74.91 \pm 0.29	75.57 \pm 0.61	83.69 (69.73)	62.22 (51.28)	62.88 (53.40)	42.62 (37.26)	

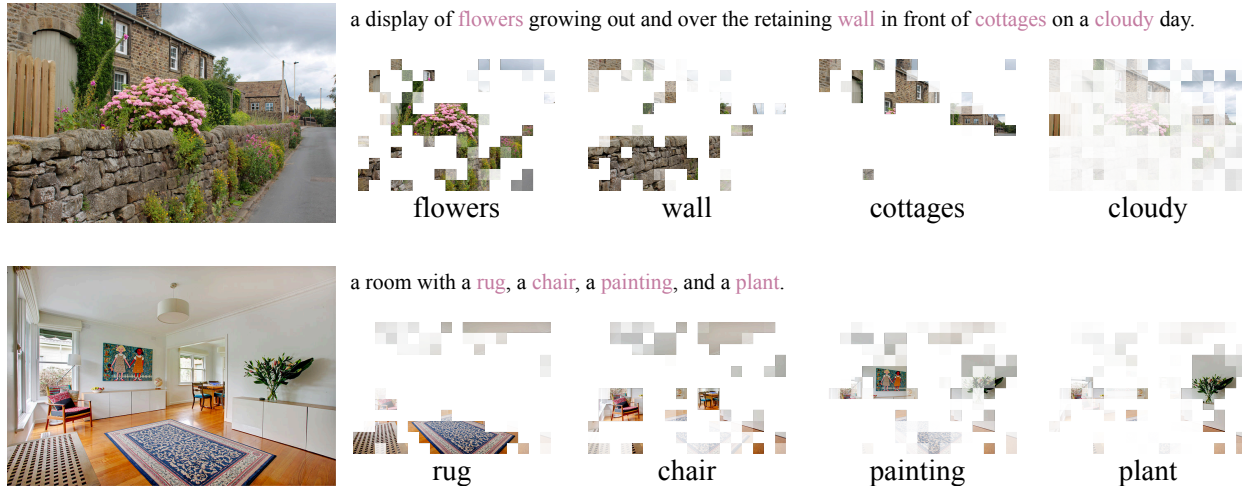


Figure 6. Visualizations

We z-normalize the plan for each token and clamp the values to $[-0.3, 0.3]$.

We can observe that mass is concentrated to a handful of tiles in a pinpointed manner in case of corporeal objects (e.g., “flower”, “rug”), and scattered over a larger area in case of a backdrop word (“cloudy”).

5. Conclusion and Future Work

In this paper, we present a minimal VLP architecture, Vision-and-Language Transformer (ViLT), and show its competence to competitors that are heavily equipped with convolutional visual embedding networks (e.g., Faster R-CNN and ResNets). We ask for future work on VLP focus more on the modality interactions inside the transformer module, rather than engaging in an arms race that merely powers up unimodal embedders.

Although remarkable as it is, ViLT-B/32 is more of a proof of concept that efficient VLP models free of convolution and region supervision can still be competent. We wrap up by pointing out a few factors that may add to the ViLT family.

Scalability. As shown in papers on large-scale transformers (Devlin et al., 2018; Dosovitskiy et al., 2020), performance of pretrained transformers scale well given appropriate amount of data. This paves the way for even better performing ViLT variants (e.g., ViLT-L (large) and ViLT-H (huge)). We leave training larger models for future work, because aligned vision-and-language datasets are yet scarce.

Masked Modeling for Visual Inputs. Considering the success of MRM, we speculate that the masked modeling objective for the visual modality helps by preserving the information up until the last layer of the transformer. However, as observed in Table 5, a naive variant of MRM on image patches (MPP) fails. We encourage future work that do not use region supervision to devise a more sophisticated masking objective for the visual modality.

Augmentation Strategies. Previous work on contrastive visual representation learning (Chen et al., 2020a;b) showed that gaussian blur, not employed by RandAugment, brings noticeable gains to downstream performance compared with a simpler augmentation strategy (He et al., 2020). Exploration of appropriate augmentation strategies for textual and visual inputs would be a great future work.

References

- Anderson, P., He, X., Buehler, C., Teney, D., Johnson, M., Gould, S., and Zhang, L. Bottom-up and top-down attention for image captioning and visual question answering. In *Proceedings of the IEEE conference on computer vision and pattern recognition*, pp. 6077–6086, 2018.
- Berman, M., Jégou, H., Vedaldi, A., Kokkinos, I., and Douze, M. Multigrain: a unified image embedding for classes and instances. *arXiv preprint arXiv:1902.05509*, 2019.
- Bugliarello, E., Cotterell, R., Okazaki, N., and Elliott, D. Multimodal pretraining unmasked: Unifying the vision and language berts. *arXiv preprint arXiv:2011.15124*, 2020.
- Chen, T., Kornblith, S., Norouzi, M., and Hinton, G. A simple framework for contrastive learning of visual representations. In *International conference on machine learning*, pp. 1597–1607. PMLR, 2020a.
- Chen, X., Fan, H., Girshick, R., and He, K. Improved baselines with momentum contrastive learning. *arXiv preprint arXiv:2003.04297*, 2020b.
- Chen, Y.-C., Li, L., Yu, L., Kholy, A. E., Ahmed, F., Gan, Z., Cheng, Y., and Liu, J. Uniter: Learning universal image-text representations. *arXiv preprint arXiv:1909.11740*, 2019.
- Cubuk, E. D., Zoph, B., Shlens, J., and Le, Q. V. Randaugment: Practical automated data augmentation with a reduced search space. In *Proceedings of the IEEE/CVF Conference on Computer Vision and Pattern Recognition Workshops*, pp. 702–703, 2020.
- Cui, Y., Che, W., Liu, T., Qin, B., Yang, Z., Wang, S., and Hu, G. Pre-training with whole word masking for chinese bert. *arXiv preprint arXiv:1906.08101*, 2019.
- Devlin, J., Chang, M.-W., Lee, K., and Toutanova, K. Bert: Pre-training of deep bidirectional transformers for language understanding. *arXiv preprint arXiv:1810.04805*, 2018.
- Dosovitskiy, A., Beyer, L., Kolesnikov, A., Weissenborn, D., Zhai, X., Unterthiner, T., Dehghani, M., Minderer, M., Heigold, G., Gelly, S., et al. An image is worth 16x16 words: Transformers for image recognition at scale. *arXiv preprint arXiv:2010.11929*, 2020.
- Faghri, F., Fleet, D. J., Kiros, J. R., and Fidler, S. Vse++: Improving visual-semantic embeddings with hard negatives. *arXiv preprint arXiv:1707.05612*, 2017.
- Gan, Z., Chen, Y.-C., Li, L., Zhu, C., Cheng, Y., and Liu, J. Large-scale adversarial training for vision-and-language representation learning. *arXiv preprint arXiv:2006.06195*, 2020.
- Goyal, Y., Khot, T., Summers-Stay, D., Batra, D., and Parikh, D. Making the v in vqa matter: Elevating the role of image understanding in visual question answering. In *Proceedings of the IEEE Conference on Computer Vision and Pattern Recognition*, pp. 6904–6913, 2017.
- He, K., Zhang, X., Ren, S., and Sun, J. Deep residual learning for image recognition. In *Proceedings of the IEEE conference on computer vision and pattern recognition*, pp. 770–778, 2016.
- He, K., Gkioxari, G., Dollár, P., and Girshick, R. Mask r-cnn. In *Proceedings of the IEEE international conference on computer vision*, pp. 2961–2969, 2017.
- He, K., Fan, H., Wu, Y., Xie, S., and Girshick, R. Momentum contrast for unsupervised visual representation learning. In *Proceedings of the IEEE/CVF Conference on Computer Vision and Pattern Recognition*, pp. 9729–9738, 2020.
- Hoffer, E., Ben-Nun, T., Hubara, I., Giladi, N., Hoefler, T., and Soudry, D. Augment your batch: Improving generalization through instance repetition. In *Proceedings of the IEEE/CVF Conference on Computer Vision and Pattern Recognition*, pp. 8129–8138, 2020.
- Hu, R., Andreas, J., Rohrbach, M., Darrell, T., and Saenko, K. Learning to reason: End-to-end module networks for visual question answering. In *Proceedings of the IEEE International Conference on Computer Vision*, pp. 804–813, 2017.
- Huang, Z., Zeng, Z., Liu, B., Fu, D., and Fu, J. Pixel-bert: Aligning image pixels with text by deep multi-modal transformers. *arXiv preprint arXiv:2004.00849*, 2020.
- Hudson, D. A. and Manning, C. D. Compositional attention networks for machine reasoning. *arXiv preprint arXiv:1803.03067*, 2018.
- Jiang, H., Misra, I., Rohrbach, M., Learned-Miller, E., and Chen, X. In defense of grid features for visual question answering. In *Proceedings of the IEEE/CVF Conference on Computer Vision and Pattern Recognition*, pp. 10267–10276, 2020.
- Karpathy, A. and Fei-Fei, L. Deep visual-semantic alignments for generating image descriptions. In *Proceedings of the IEEE conference on computer vision and pattern recognition*, pp. 3128–3137, 2015.

- Krishna, R., Zhu, Y., Groth, O., Johnson, J., Hata, K., Kravitz, J., Chen, S., Kalantidis, Y., Li, L.-J., Shamma, D. A., et al. Visual genome: Connecting language and vision using crowdsourced dense image annotations. *International journal of computer vision*, 123(1):32–73, 2017.
- Krizhevsky, A., Sutskever, I., and Hinton, G. E. Imagenet classification with deep convolutional neural networks. In *NIPS*, 2012.
- Kuznetsova, A., Rom, H., Alldrin, N., Uijlings, J., Krasin, I., Pont-Tuset, J., Kamali, S., Popov, S., Mallocci, M., Kolesnikov, A., et al. The open images dataset v4. *International Journal of Computer Vision*, pp. 1–26, 2020.
- Lee, K.-H., Chen, X., Hua, G., Hu, H., and He, X. Stacked cross attention for image-text matching. In *Proceedings of the European Conference on Computer Vision (ECCV)*, pp. 201–216, 2018.
- Li, G., Duan, N., Fang, Y., Gong, M., Jiang, D., and Zhou, M. Unicoder-vl: A universal encoder for vision and language by cross-modal pre-training. In *AAAI*, pp. 11336–11344, 2020a.
- Li, L. H., Yatskar, M., Yin, D., Hsieh, C.-J., and Chang, K.-W. Visualbert: A simple and performant baseline for vision and language. *arXiv preprint arXiv:1908.03557*, 2019.
- Li, X., Yin, X., Li, C., Zhang, P., Hu, X., Zhang, L., Wang, L., Hu, H., Dong, L., Wei, F., et al. Oscar: Object-semantic aligned pre-training for vision-language tasks. In *European Conference on Computer Vision*, pp. 121–137. Springer, 2020b.
- Lin, T.-Y., Maire, M., Belongie, S., Hays, J., Perona, P., Ramanan, D., Dollár, P., and Zitnick, C. L. Microsoft coco: Common objects in context. In *European conference on computer vision*, pp. 740–755. Springer, 2014.
- Loshchilov, I. and Hutter, F. Decoupled weight decay regularization. *arXiv preprint arXiv:1711.05101*, 2017.
- Lu, J., Batra, D., Parikh, D., and Lee, S. Vilbert: Pretraining task-agnostic visiolinguistic representations for vision-and-language tasks. In *Advances in Neural Information Processing Systems*, pp. 13–23, 2019.
- Lu, J., Goswami, V., Rohrbach, M., Parikh, D., and Lee, S. 12-in-1: Multi-task vision and language representation learning. In *Proceedings of the IEEE/CVF Conference on Computer Vision and Pattern Recognition*, pp. 10437–10446, 2020.
- Nguyen, D.-K., Goswami, V., and Chen, X. Revisiting modulated convolutions for visual counting and beyond. *arXiv preprint arXiv:2004.11883*, 2020.
- Ordonez, V., Kulkarni, G., and Berg, T. Im2text: Describing images using 1 million captioned photographs. *Advances in neural information processing systems*, 24:1143–1151, 2011.
- Perez, E., Strub, F., De Vries, H., Dumoulin, V., and Courville, A. Film: Visual reasoning with a general conditioning layer. In *Proceedings of the AAAI Conference on Artificial Intelligence*, volume 32, 2018.
- Plummer, B. A., Wang, L., Cervantes, C. M., Caicedo, J. C., Hockenmaier, J., and Lazebnik, S. Flickr30k entities: Collecting region-to-phrase correspondences for richer image-to-sentence models. In *Proceedings of the IEEE international conference on computer vision*, pp. 2641–2649, 2015.
- Qi, D., Su, L., Song, J., Cui, E., Bharti, T., and Sacheti, A. Imagebert: Cross-modal pre-training with large-scale weak-supervised image-text data. *arXiv preprint arXiv:2001.07966*, 2020.
- Radford, A., Sutskever, I., Kim, J., Krueger, G., and Agarwal, S. Learning transferable visual models from natural language supervision, 2021.
- Ren, S., He, K., Girshick, R., and Sun, J. Faster r-cnn: Towards real-time object detection with region proposal networks. *IEEE transactions on pattern analysis and machine intelligence*, 39(6):1137–1149, 2016.
- Russakovsky, O., Deng, J., Su, H., Krause, J., Satheesh, S., Ma, S., Huang, Z., Karpathy, A., Khosla, A., Bernstein, M., et al. Imagenet large scale visual recognition challenge. *International journal of computer vision*, 115(3): 211–252, 2015.
- Sharma, P., Ding, N., Goodman, S., and Soricut, R. Conceptual captions: A cleaned, hypernymed, image alt-text dataset for automatic image captioning. In *Proceedings of the 56th Annual Meeting of the Association for Computational Linguistics (Volume 1: Long Papers)*, pp. 2556–2565, 2018.
- Shorten, C. and Khoshgoftaar, T. M. A survey on image data augmentation for deep learning. *Journal of Big Data*, 6(1):1–48, 2019.
- Su, W., Zhu, X., Cao, Y., Li, B., Lu, L., Wei, F., and Dai, J. Vi-ber: Pre-training of generic visual-linguistic representations. *arXiv preprint arXiv:1908.08530*, 2019.
- Suhr, A., Zhou, S., Zhang, A., Zhang, I., Bai, H., and Artzi, Y. A corpus for reasoning about natural language grounded in photographs. *arXiv preprint arXiv:1811.00491*, 2018.

- Tan, H. and Bansal, M. Lxmert: Learning cross-modality encoder representations from transformers. *arXiv preprint arXiv:1908.07490*, 2019.
- Touvron, H., Cord, M., Douze, M., Massa, F., Sablayrolles, A., and Jégou, H. Training data-efficient image transformers & distillation through attention. *arXiv preprint arXiv:2012.12877*, 2020.
- Vaswani, A., Shazeer, N., Parmar, N., Uszkoreit, J., Jones, L., Gomez, A. N., Kaiser, Ł., and Polosukhin, I. Attention is all you need. *Advances in neural information processing systems*, 30:5998–6008, 2017.
- Xie, S., Girshick, R., Dollár, P., Tu, Z., and He, K. Aggregated residual transformations for deep neural networks. In *Proceedings of the IEEE conference on computer vision and pattern recognition*, pp. 1492–1500, 2017.
- Xie, Y., Wang, X., Wang, R., and Zha, H. A fast proximal point method for computing exact wasserstein distance. In *Uncertainty in Artificial Intelligence*, pp. 433–453. PMLR, 2020.
- Yu, F., Tang, J., Yin, W., Sun, Y., Tian, H., Wu, H., and Wang, H. Ernie-vil: Knowledge enhanced vision-language representations through scene graph. *arXiv preprint arXiv:2006.16934*, 2020.
- Yu, Z., Yu, J., Cui, Y., Tao, D., and Tian, Q. Deep modular co-attention networks for visual question answering. In *Proceedings of the IEEE/CVF Conference on Computer Vision and Pattern Recognition*, pp. 6281–6290, 2019.
- Yun, S., Han, D., Oh, S. J., Chun, S., Choe, J., and Yoo, Y. Cutmix: Regularization strategy to train strong classifiers with localizable features. In *Proceedings of the IEEE/CVF International Conference on Computer Vision*, pp. 6023–6032, 2019.
- Zhang, H., Cisse, M., Dauphin, Y. N., and Lopez-Paz, D. mixup: Beyond empirical risk minimization. *arXiv preprint arXiv:1710.09412*, 2017.
- Zhang, P., Li, X., Hu, X., Yang, J., Zhang, L., Wang, L., Choi, Y., and Gao, J. Vinvl: Making visual representations matter in vision-language models. *arXiv preprint arXiv:2101.00529*, 2021.
- Zhou, L., Palangi, H., Zhang, L., Hu, H., Corso, J. J., and Gao, J. Unified vision-language pre-training for image captioning and vqa. In *AAAI*, pp. 13041–13049, 2020.